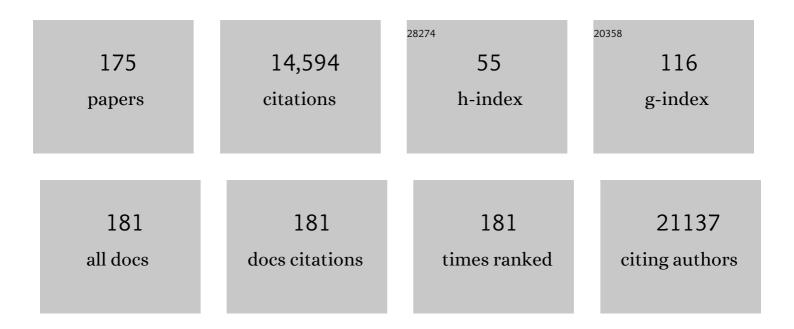
Jianliang Shen

List of Publications by Year in descending order

Source: https://exaly.com/author-pdf/7050686/publications.pdf Version: 2024-02-01



LIANLIANC SHEN

#	Article	IF	CITATIONS
1	Principles of nanoparticle design for overcoming biological barriers to drug delivery. Nature Biotechnology, 2015, 33, 941-951.	17.5	4,868
2	XBP1 promotes triple-negative breast cancer by controlling the HIF1α pathway. Nature, 2014, 508, 103-107.	27.8	663
3	New genes involved in cancer identified by retroviral tagging. Nature Genetics, 2002, 32, 166-174.	21.4	393
4	Safety of Nanoparticles in Medicine. Current Drug Targets, 2015, 16, 1671-1681.	2.1	384
5	An injectable nanoparticle generator enhances delivery of cancer therapeutics. Nature Biotechnology, 2016, 34, 414-418.	17.5	248
6	Leukaemia disease genes: large-scale cloning and pathway predictions. Nature Genetics, 1999, 23, 348-353.	21.4	221
7	Multifunctional magnetic iron oxide nanoparticles: an advanced platform for cancer theranostics. Theranostics, 2020, 10, 6278-6309.	10.0	213
8	Immunoregulation in Diabetic Wound Repair with a Photoenhanced Glycyrrhizic Acid Hydrogel Scaffold. Advanced Materials, 2022, 34, e2200521.	21.0	212
9	Engineering Robust Agâ€Decorated Polydopamine Nanoâ€Photothermal Platforms to Combat Bacterial Infection and Prompt Wound Healing. Advanced Science, 2022, 9, e2106015.	11.2	198
10	Pharmacological targeting of MYC-regulated IRE1/XBP1 pathway suppresses MYC-driven breast cancer. Journal of Clinical Investigation, 2018, 128, 1283-1299.	8.2	163
11	Cyclodextrin and Polyethylenimine Functionalized Mesoporous Silica Nanoparticles for Delivery of siRNA Cancer Therapeutics. Theranostics, 2014, 4, 487-497.	10.0	161
12	The nano-plasma interface: Implications of the protein corona. Colloids and Surfaces B: Biointerfaces, 2014, 124, 17-24.	5.0	155
13	The CDS1 Gene Encoding CDP-diacylglycerol Synthase In Saccharomyces cerevisiae Is Essential for Cell Growth. Journal of Biological Chemistry, 1996, 271, 789-795.	3.4	142
14	Mussel-inspired agarose hydrogel scaffolds for skin tissue engineering. Bioactive Materials, 2021, 6, 579-588.	15.6	142
15	Polydopamine nanoparticle-dotted food gum hydrogel with excellent antibacterial activity and rapid shape adaptability for accelerated bacteria-infected wound healing. Bioactive Materials, 2021, 6, 2647-2657.	15.6	142
16	Facile formation of injectable quaternized chitosan/tannic acid hydrogels with antibacterial and ROS scavenging capabilities for diabetic wound healing. International Journal of Biological Macromolecules, 2022, 195, 190-197.	7.5	135
17	Lipopolyplex potentiates anti-tumor immunity of mRNA-based vaccination. Biomaterials, 2017, 125, 81-89.	11.4	128
18	Polyethylene glycol (PEG)-dendron phospholipids as innovative constructs for the preparation of super stealth liposomes for anticancer therapy. Journal of Controlled Release, 2015, 199, 106-113.	9.9	125

#	Article	IF	CITATIONS
19	Targeting Autocrine CCL5–CCR5 Axis Reprograms Immunosuppressive Myeloid Cells and Reinvigorates Antitumor Immunity. Cancer Research, 2017, 77, 2857-2868.	0.9	111
20	High Capacity Nanoporous Silicon Carrier for Systemic Delivery of Gene Silencing Therapeutics. ACS Nano, 2013, 7, 9867-9880.	14.6	110
21	<i>SMAD4</i> Gene Mutation Renders Pancreatic Cancer Resistance to Radiotherapy through Promotion of Autophagy. Clinical Cancer Research, 2018, 24, 3176-3185.	7.0	109
22	A Liposome Encapsulated Ruthenium Polypyridine Complex as a Theranostic Platform for Triple-Negative Breast Cancer. Nano Letters, 2017, 17, 2913-2920.	9.1	107
23	Polydopamine/montmorillonite-embedded pullulan hydrogels as efficient adsorbents for removing crystal violet. Journal of Hazardous Materials, 2021, 402, 123359.	12.4	107
24	Enhancing Chemotherapy Response with Sustained EphA2 Silencing Using Multistage Vector Delivery. Clinical Cancer Research, 2013, 19, 1806-1815.	7.0	105
25	Engineering functional inorganic–organic hybrid systems: advances in siRNA therapeutics. Chemical Society Reviews, 2018, 47, 1969-1995.	38.1	105
26	Cyclic cRGDfk peptide and Chlorin e6 functionalized silk fibroin nanoparticles for targeted drug delivery and photodynamic therapy. Biomaterials, 2018, 161, 306-320.	11.4	102
27	Targeting RPL39 and MLF2 reduces tumor initiation and metastasis in breast cancer by inhibiting nitric oxide synthase signaling. Proceedings of the National Academy of Sciences of the United States of America, 2014, 111, 8838-8843.	7.1	99
28	Advances in nanomaterials for use in photothermal and photodynamic therapeutics (Review). Molecular Medicine Reports, 2019, 20, 5-15.	2.4	99
29	Hesperetin impairs glucose uptake and inhibits proliferation of breast cancer cells. Cell Biochemistry and Function, 2013, 31, 374-379.	2.9	97
30	Multifunctional Gold Nanorods for siRNA Gene Silencing and Photothermal Therapy. Advanced Healthcare Materials, 2014, 3, 1629-1637.	7.6	97
31	Shrinkage of pegylated and non-pegylated liposomes in serum. Colloids and Surfaces B: Biointerfaces, 2014, 114, 294-300.	5.0	96
32	Removal of copper ions from water using polysaccharide-constructed hydrogels. Carbohydrate Polymers, 2019, 209, 101-110.	10.2	93
33	Ratiometric and colorimetric fluorescent probe for hypochlorite monitor and application for bioimaging in living cells, bacteria and zebrafish. Journal of Hazardous Materials, 2020, 388, 122029.	12.4	91
34	Porous Silicon Microparticle Potentiates Anti-Tumor Immunity by Enhancing Cross-Presentation and Inducing Type I Interferon Response. Cell Reports, 2015, 11, 957-966.	6.4	90
35	Metformin Liposome-Mediated PD-L1 Downregulation for Amplifying the Photodynamic Immunotherapy Efficacy. ACS Applied Materials & Interfaces, 2021, 13, 8026-8041.	8.0	87
36	A Vehicleâ€Free Antimicrobial Polymer Hybrid Gold Nanoparticle as Synergistically Therapeutic Platforms for <i>Staphylococcus aureus</i> Infected Wound Healing. Advanced Science, 2022, 9, e2105223.	11.2	87

#	Article	IF	CITATIONS
37	Cooperative, Nanoparticleâ€Enabled Thermal Therapy of Breast Cancer. Advanced Healthcare Materials, 2012, 1, 84-89.	7.6	85
38	Salecan polysaccharide-based hydrogels and their applications: a review. Journal of Materials Chemistry B, 2019, 7, 2577-2587.	5.8	83
39	Efficient Decontamination of Lead Ions from Wastewater by Salecan Polysaccharide-Based Hydrogels. ACS Sustainable Chemistry and Engineering, 2019, 7, 11014-11023.	6.7	82
40	Evaluation of anticancer activity of celastrol liposomes in prostate cancer cells. Journal of Microencapsulation, 2014, 31, 501-507.	2.8	80
41	Mild Hyperthermia-Assisted ROS Scavenging Hydrogels Achieve Diabetic Wound Healing. ACS Macro Letters, 2022, 11, 861-867.	4.8	80
42	Radio-photothermal therapy mediated by a single compartment nanoplatform depletes tumor initiating cells and reduces lung metastasis in the orthotopic 4T1 breast tumor model. Nanoscale, 2015, 7, 19438-19447.	5.6	78
43	Contribution of Kupffer cells to liposome accumulation in the liver. Colloids and Surfaces B: Biointerfaces, 2017, 158, 356-362.	5.0	78
44	ε‑Polylysine-stabilized agarose/polydopamine hydrogel dressings with robust photothermal property for wound healing. Carbohydrate Polymers, 2021, 264, 118046.	10.2	78
45	Macroporous Hydrogel Scaffolds with Tunable Physicochemical Properties for Tissue Engineering Constructed Using Renewable Polysaccharides. ACS Applied Materials & Interfaces, 2020, 12, 13256-13264.	8.0	75
46	Facile formation of salecan/agarose hydrogels with tunable structural properties for cell culture. Carbohydrate Polymers, 2019, 224, 115208.	10.2	70
47	Polydopamine-incorporated dextran hydrogel drug carrier with tailorable structure for wound healing. Carbohydrate Polymers, 2021, 253, 117213.	10.2	68
48	MicroRNA-34a: Potent Tumor Suppressor, Cancer Stem Cell Inhibitor, and Potential Anticancer Therapeutic. Frontiers in Cell and Developmental Biology, 2021, 9, 640587.	3.7	67
49	Multistage Vectored siRNA Targeting Ataxiaâ€Telangiectasia Mutated for Breast Cancer Therapy. Small, 2013, 9, 1799-1808.	10.0	64
50	Efficient decontamination of heavy metals from aqueous solution using pullulan/polydopamine hydrogels. International Journal of Biological Macromolecules, 2020, 145, 1049-1058.	7.5	63
51	Nanoplatforms for mRNA Therapeutics. Advanced Therapeutics, 2021, 4, .	3.2	62
52	Activation of the Rap1 Guanine Nucleotide Exchange Gene,CalDAG-GEF I, in BXH-2 Murine Myeloid Leukemia. Journal of Biological Chemistry, 2001, 276, 11804-11811.	3.4	61
53	Tumor vascular permeabilization using localized mild hyperthermia to improve macromolecule transport. Nanomedicine: Nanotechnology, Biology, and Medicine, 2014, 10, 1487-1496.	3.3	58
54	Multi-step encapsulation of chemotherapy and gene silencing agents in functionalized mesoporous silica nanoparticles. Nanoscale, 2017, 9, 5329-5341.	5.6	58

#	Article	IF	CITATIONS
55	Targeted drug delivery for tumor therapy inside the bone marrow. Biomaterials, 2018, 155, 191-202.	11.4	57
56	Mild Hyperthermia Enhances Transport of Liposomal Gemcitabine and Improves In Vivo Therapeutic Response. Advanced Healthcare Materials, 2015, 4, 1092-1103.	7.6	56
57	Theory and Experimental Validation of a Spatio-temporal Model of Chemotherapy Transport to Enhance Tumor Cell Kill. PLoS Computational Biology, 2016, 12, e1004969.	3.2	55
58	A novel dual-response chemosensor for bioimaging of Exogenous/Endogenous hypochlorite and hydrazine in living cells, Pseudomonas aeruginosa and zebrafish. Sensors and Actuators B: Chemical, 2020, 321, 128450.	7.8	55
59	Growth of Cu ₂ O Nanoparticles on Two-Dimensional Zr–Ferrocene–Metal–Organic Framework Nanosheets for Photothermally Enhanced Chemodynamic Antibacterial Therapy. Inorganic Chemistry, 2022, 61, 9328-9338.	4.0	55
60	Comparison of three water-soluble polyphosphate tripolyphosphate, phytic acid, and sodium hexametaphosphate as crosslinking agents in chitosan nanoparticle formulation. Carbohydrate Polymers, 2020, 230, 115577.	10.2	54
61	Estrogen Receptor α Regulates ATM Expression through miRNAs in Breast Cancer. Clinical Cancer Research, 2013, 19, 4994-5002.	7.0	53
62	Co-delivery of tumor antigen and dual toll-like receptor ligands into dendritic cell by silicon microparticle enables efficient immunotherapy against melanoma. Journal of Controlled Release, 2018, 272, 72-82.	9.9	53
63	Highly efficient dye decontamination via microbial salecan polysaccharide-based gels. Carbohydrate Polymers, 2019, 219, 1-11.	10.2	53
64	Multistage vector (MSV) therapeutics. Journal of Controlled Release, 2015, 219, 406-415.	9.9	52
65	Recent Advances in Discovering the Role of CCL5 in Metastatic Breast Cancer. Mini-Reviews in Medicinal Chemistry, 2015, 15, 1063-1072.	2.4	52
66	Construction of macroporous salecan polysaccharide-based adsorbents for wastewater remediation. International Journal of Biological Macromolecules, 2019, 132, 429-438.	7.5	51
67	Construction of functional curdlan hydrogels with bio-inspired polydopamine for synergistic periodontal antibacterial therapeutics. Carbohydrate Polymers, 2020, 245, 116585.	10.2	51
68	Polycation-functionalized nanoporous silicon particles for gene silencing on breast cancer cells. Biomaterials, 2014, 35, 423-431.	11.4	49
69	Bone marrow endothelium-targeted therapeutics for metastatic breast cancer. Journal of Controlled Release, 2014, 187, 22-29.	9.9	47
70	Enzyme-responsive multistage vector for drug delivery to tumor tissue. Pharmacological Research, 2016, 113, 92-99.	7.1	47
71	Post-nano strategies for drug delivery: multistage porous silicon microvectors. Journal of Materials Chemistry B, 2017, 5, 207-219.	5.8	47
72	Combination Therapy of Doxorubicin and Quercetin on Multidrug-Resistant Breast Cancer and Their Sequential Delivery by Reduction-Sensitive Hyaluronic Acid-Based Conjugate/ <scp>d</scp> -α-Tocopheryl Poly(ethylene glycol) 1000 Succinate Mixed Micelles. Molecular Pharmaceutics, 2020, 17, 1415-1427.	4.6	46

#	Article	IF	CITATIONS
73	Symmetrical bis-salophen probe serves as a selectively and sensitively fluorescent switch of gallium ions in living cells and zebrafish. Talanta, 2019, 205, 120118.	5.5	45
74	Sustainable, flexible and biocompatible hydrogels derived from microbial polysaccharides with tailorable structures for tissue engineering. Carbohydrate Polymers, 2020, 237, 116160.	10.2	45
75	A Micro/Nano Composite for Combination Treatment of Melanoma Lung Metastasis. Advanced Healthcare Materials, 2016, 5, 936-946.	7.6	44
76	Taking the vehicle out of drug delivery. Materials Today, 2017, 20, 95-97.	14.2	44
77	A Novel DNA Aptamer for Dual Targeting of Polymorphonuclear Myeloid-derived Suppressor Cells and Tumor Cells. Theranostics, 2018, 8, 31-44.	10.0	44
78	Nanochannel Technology for Constant Delivery of Chemotherapeutics: Beyond Metronomic Administration. Pharmaceutical Research, 2011, 28, 292-300.	3.5	43
79	Hesperetin: An inhibitor of the transforming growth factor-β (TGF-β) signaling pathway. European Journal of Medicinal Chemistry, 2012, 58, 390-395.	5.5	40
80	Multistage vector delivery of sulindac and silymarin for prevention of colon cancer. Colloids and Surfaces B: Biointerfaces, 2015, 136, 694-703.	5.0	39
81	Hesperetin Liposomes for Cancer Therapy. Current Drug Delivery, 2016, 13, 711-719.	1.6	39
82	Strategies for improving drug delivery: nanocarriers and microenvironmental priming. Expert Opinion on Drug Delivery, 2017, 14, 865-877.	5.0	39
83	Biocompatible Hydrogels Based on Food Gums with Tunable Physicochemical Properties as Scaffolds for Cell Culture. Journal of Agricultural and Food Chemistry, 2020, 68, 3770-3778.	5.2	39
84	Metallic phase enabling MoS2 nanosheets as an efficient sonosensitizer for photothermal-enhanced sonodynamic antibacterial therapy. Journal of Nanobiotechnology, 2022, 20, 136.	9.1	38
85	Regulation of Phospholipid Biosynthetic Enzymes by the Level of CDP-Diacylglycerol Synthase Activity. Journal of Biological Chemistry, 1997, 272, 11215-11220.	3.4	37
86	Label-Free Isothermal Amplification Assay for Specific and Highly Sensitive Colorimetric miRNA Detection. ACS Omega, 2016, 1, 448-455.	3.5	36
87	PTGER3 induces ovary tumorigenesis and confers resistance to cisplatin therapy through up-regulation Ras-MAPK/Erk-ETS1-ELK1/CFTR1 axis. EBioMedicine, 2019, 40, 290-304.	6.1	36
88	ESIPT-based fluorescent probe for bioimaging and identification of group IIIA ions in live cells and zebrafish. Bioorganic Chemistry, 2021, 109, 104746.	4.1	36
89	Highly sensitive and selective light-up fluorescent probe for monitoring gallium and chromium ions <i>in vitro</i> and <i>in vivo</i> . Analyst, The, 2019, 144, 3807-3816.	3.5	35
90	Insight into triphenylamine and coumarin serving as copper (II) sensors with "OFF―strategy and for bio-imaging in living cells. Spectrochimica Acta - Part A: Molecular and Biomolecular Spectroscopy, 2020, 224, 117384.	3.9	33

#	Article	IF	CITATIONS
91	Surface engineering on mesoporous silica chips for enriching low molecular weight phosphorylated proteins. Nanoscale, 2011, 3, 421-428.	5.6	32
92	Circulating Proteolytic Products of Carboxypeptidase N for Early Detection of Breast Cancer. Clinical Chemistry, 2014, 60, 233-242.	3.2	31
93	Geometrical confinement of Gd(DOTA) molecules within mesoporous silicon nanoconstructs for MR imaging of cancer. Cancer Letters, 2014, 352, 97-101.	7.2	31
94	Systemic Delivery of Aptamer-Conjugated XBP1 siRNA Nanoparticles for Efficient Suppression of HER2+ Breast Cancer. ACS Applied Materials & Interfaces, 2020, 12, 32360-32371.	8.0	30
95	Selectively down-regulated PD-L1 by albumin-phenformin nanoparticles mediated mitochondrial dysfunction to stimulate tumor-specific immunological response for enhanced mild-temperature photothermal efficacy. Journal of Nanobiotechnology, 2021, 19, 375.	9.1	30
96	Tyrosine kinase inhibitors induce mesenchymal stem cell–mediated resistance in BCR-ABL+ acute lymphoblastic leukemia. Blood, 2015, 125, 2968-2973.	1.4	29
97	Enhancing cancer immunotherapy through nanotechnology-mediated tumor infiltration and activation of immune cells. Seminars in Immunology, 2017, 34, 114-122.	5.6	29
98	Reaction-Based Ratiometric and Colorimetric Chemosensor for Bioimaging of Biosulfite in Live Cells, Zebrafish, and Food Samples. Journal of Agricultural and Food Chemistry, 2020, 68, 11774-11781.	5.2	29
99	Reversible Chemosensor for Bioimaging and Biosensing of Zn(II) and hpH in Cells, Larval Zebrafish, and Plants with Dual-Channel Fluorescence Signals. Inorganic Chemistry, 2021, 60, 5563-5572.	4.0	29
100	The ICT-based fluorescence and colorimetric dual sensing of endogenous hypochlorite in living cells, bacteria, and zebrafish. Analyst, The, 2020, 145, 29-33.	3.5	28
101	Chitosan oligosaccharide regulates AMPK and STAT1 pathways synergistically to mediate PD-L1 expression for cancer chemoimmunotherapy. Carbohydrate Polymers, 2022, 277, 118869.	10.2	28
102	Hollow covalent organic framework-sheltering CRISPR/Cas12a as an in-vivo nanosensor for ATP imaging. Biosensors and Bioelectronics, 2022, 209, 114239.	10.1	28
103	Mitochondria-Targeted Chemosensor to Discriminately and Continuously Visualize HClO and H ₂ S with Multiresponse Fluorescence Signals for <i>In Vitro</i> and <i>In Vivo</i> Bioimaging. ACS Applied Bio Materials, 2020, 3, 7886-7897.	4.6	27
104	A facile assay for rapid detection of COVID-19 antibodies. RSC Advances, 2020, 10, 28041-28048.	3.6	26
105	A dual-functional chitosan derivative platform for fungal keratitis. Carbohydrate Polymers, 2022, 275, 118762.	10.2	26
106	Reduction of CDP-diacylglycerol Synthase Activity Results in the Excretion of Inositol by Saccharomyces cerevisiae. Journal of Biological Chemistry, 1996, 271, 29043-29048.	3.4	25
107	Architecting polyelectrolyte hydrogels with Cu-assisted polydopamine nanoparticles for photothermal antibacterial therapy. Materials Today Bio, 2022, 15, 100264.	5.5	25
108	Bone-targeting nanoparticle to co-deliver decitabine and arsenic trioxide for effective therapy of myelodysplastic syndrome with low systemic toxicity. Journal of Controlled Release, 2017, 268, 92-101.	9.9	24

#	Article	IF	CITATIONS
109	Chemotherapy Sensitizes Therapy-Resistant Cells to Mild Hyperthermia by Suppressing Heat Shock Protein 27 Expression in Triple-Negative Breast Cancer. Clinical Cancer Research, 2018, 24, 4900-4912.	7.0	24
110	FRET-based colorimetric and ratiometric sensor for visualizing pH change and application for bioimaging in living cells, bacteria and zebrafish. Analytica Chimica Acta, 2020, 1127, 29-38.	5.4	24
111	Regulation of Phosphatidylglycerophosphate Synthase Levels inSaccharomyces cerevisiae. Journal of Biological Chemistry, 1998, 273, 11638-11642.	3.4	22
112	The Sox4/Tcf7l1 axis promotes progression of BCR-ABL-positive acute lymphoblastic leukemia. Haematologica, 2014, 99, 1591-1598.	3.5	22
113	Execution of aggregation-induced emission as nano-sensors for hypochlorite detection and application for bioimaging in living cells and zebrafish. Talanta, 2020, 214, 120842.	5.5	22
114	Polyarginine Induces an Antitumor Immune Response through Binding to Toll‣ike Receptor 4. Small, 2014, 10, 1250-1254.	10.0	21
115	An IKKα-Nucleophosmin Axis Utilizes Inflammatory Signaling to Promote Genome Integrity. Cell Reports, 2013, 5, 1243-1255.	6.4	20
116	Development of targeted therapy therapeutics to sensitize triple-negative breast cancer chemosensitivity utilizing bacteriophage phi29 derived packaging RNA. Journal of Nanobiotechnology, 2021, 19, 13.	9.1	20
117	Zinc oxide end-capped Fe ₃ O ₄ @mSiO ₂ core-shell nanocarriers as targeted and responsive drug delivery system for chemo-/ions synergistic therapeutics. Drug Delivery, 2019, 26, 732-743.	5.7	18
118	Synergistic Activation of Antitumor Immunity by a Particulate Therapeutic Vaccine. Advanced Science, 2021, 8, 2100166.	11.2	18
119	Activation of Clg, a Novel Dbl Family Guanine Nucleotide Exchange Factor Gene, by Proviral Insertion atEvi24, a Common Integration Site in B Cell and Myeloid Leukemias. Journal of Biological Chemistry, 2002, 277, 13463-13472.	3.4	17
120	Serum peptidomic biomarkers for pulmonary metastatic melanoma identified by means of a nanopore-based assay. Cancer Letters, 2013, 334, 202-210.	7.2	17
121	Sequential deconstruction of composite drug transport in metastatic breast cancer. Science Advances, 2020, 6, eaba4498.	10.3	17
122	A novel strategy for rhodamine B-based fluorescent probes with a selective glutathione response for bioimaging in living cells. Analyst, The, 2020, 145, 4239-4244.	3.5	17
123	Molecular targeting of FATP4 transporter for oral delivery of therapeutic peptide. Science Advances, 2020, 6, eaba0145.	10.3	16
124	Highly sensitive fluorescent sensor based on coumarin organic dye for pyrophosphate ion turn-on biosensing in synovial fluid. Spectrochimica Acta - Part A: Molecular and Biomolecular Spectroscopy, 2021, 257, 119792.	3.9	15
125	Human Equilibrative Nucleoside Transporter-1 Knockdown Tunes Cellular Mechanics through Epithelial-Mesenchymal Transition in Pancreatic Cancer Cells. PLoS ONE, 2014, 9, e107973.	2.5	14
126	DNA Thioaptamer with Homing Specificity to Lymphoma Bone Marrow Involvement. Molecular Pharmaceutics, 2018, 15, 1814-1825.	4.6	13

#	Article	IF	CITATIONS
127	FRET-based sensor for visualizing pH variation with colorimetric/ratiometric strategy and application for bioimaging in living cells, bacteria and zebrafish. Analyst, The, 2020, 145, 4283-4294.	3.5	13
128	Facile preparation of one-dimensional nanostructures through polymerization-induced self-assembly mediated by host–guest interaction. Polymer Chemistry, 2020, 11, 4208-4212.	3.9	13
129	Directed arrangement of siRNA <i>via</i> polymerization-induced electrostatic self-assembly. Chemical Communications, 2020, 56, 2411-2414.	4.1	13
130	Transient Mild Hyperthermia Induces E-selectin Mediated Localization of Mesoporous Silicon Vectors in Solid Tumors. PLoS ONE, 2014, 9, e86489.	2.5	13
131	Common Sites of Retroviral Integration in Mouse Hematopoietic Tumors Identified by High-Throughput, Single Nucleotide Polymorphism-Based Mapping and Bacterial Artificial Chromosome Hybridization. Journal of Virology, 2003, 77, 1584-1588.	3.4	12
132	Circulating Peptidome to Indicate the Tumor-resident Proteolysis. Scientific Reports, 2015, 5, 9327.	3.3	12
133	Immunotherapeutic Transport Oncophysics: Space, Time, and Immune Activation in Cancer. Trends in Cancer, 2020, 6, 40-48.	7.4	12
134	A novel ratiometric and colorimetric chemosensor for highly sensitive, selective and ultrafast tracing of HClO in live cells, bacteria and zebrafish. Analytica Chimica Acta, 2021, 1161, 338472.	5.4	12
135	In Situ Forming Hydrogel as a Tracer and Degradable Lacrimal Plug for Dry Eye Treatment. Advanced Healthcare Materials, 2022, 11, .	7.6	12
136	Distribution of Glutathione-Stabilized Gold Nanoparticles in Feline Fibrosarcomas and Their Role as a Drug Delivery System for Doxorubicin—Preclinical Studies in a Murine Model. International Journal of Molecular Sciences, 2018, 19, 1021.	4.1	11
137	Virusâ€Mimic mRNA Vaccine for Cancer Treatment. Advanced Therapeutics, 2021, 4, 2100144.	3.2	11
138	Charge Regulation of Self-Assembled Tubules by Protonation for Efficiently Selective and Controlled Drug Delivery. IScience, 2019, 19, 224-231.	4.1	10
139	Mesoporous Silica Coating on Carbon Nanotubes: Layer-by-Layer Method. Langmuir, 2013, 29, 6815-6822.	3.5	9
140	Targeted Delivery of Shear Stress-Inducible microRNAs by Nanoparticles to Prevent Vulnerable Atherosclerotic Lesions. Methodist DeBakey Cardiovascular Journal, 2021, 12, 152.	1.0	8
141	Investigation of parameters that determine Nano-DC vaccine transport. Biomedical Microdevices, 2019, 21, 39.	2.8	8
142	Reaction-based chemosensor as dual-channel indicator for visualizing and bioimaging of exogenous hypochlorite concentrations in living cells, Pseudomonas aeruginosa, and zebrafish. Analytica Chimica Acta, 2021, 1157, 338391.	5.4	8
143	A newly nitrobenzoxadiazole (NBD)-fused reversible fluorescence probe for pH monitoring and application in bioimaging. Talanta, 2021, 228, 122218.	5.5	8
144	Integrating the second near-infrared fluorescence imaging with clinical techniques for multimodal cancer imaging by neodymiumdoped gadolinium tungstate nanoparticles. Nano Research, 2021, 14, 2160.	10.4	8

4.1

3

#	Article	IF	CITATIONS
145	Liveâ€cell singleâ€molecule imaging reveals clathrin and caveolinâ€1 dependent docking of SMAD4 at the cell membrane. FEBS Letters, 2013, 587, 3912-3920.	2.8	7
146	A pyruvate decarboxylase-mediated therapeutic strategy for mimicking yeast metabolism in cancer cells. Pharmacological Research, 2016, 111, 413-421.	7.1	7
147	Systematic comparison of methods for determining the in vivo biodistribution of porous nanostructured injectable inorganic particles. Acta Biomaterialia, 2019, 97, 501-512.	8.3	7
148	3D CoPt nanostructures hybridized with iridium complexes for multimodal imaging and combined photothermal-chemotherapy. Journal of Inorganic Biochemistry, 2021, 219, 111429.	3.5	7
149	Novel Multistage Nanoparticle Drug Delivery to Ablate Leukemia Stem Cells in Their Niche Blood, 2012, 120, 2631-2631.	1.4	7
150	BODIPY-based rapid response fluorescence probe for sensing and bioimaging endogenous superoxide anion in living cells. Spectrochimica Acta - Part A: Molecular and Biomolecular Spectroscopy, 2022, 269, 120766.	3.9	7
151	Synthesis, biological evaluation and molecular docking of 4-Amino-2H-benzo[h]chromen-2-one (ABO) analogs containing the piperazine moiety. Bioorganic and Medicinal Chemistry, 2019, 27, 115081.	3.0	6
152	Editorial: Supramolecular Nanomaterials for Engineering, Drug Delivery, and Medical Applications. Frontiers in Chemistry, 2020, 8, 626468.	3.6	6
153	Directional effect on the fusion of ellipsoidal morphologies into nanorods and nanotubes. RSC Advances, 2021, 11, 1729-1735.	3.6	6
154	Simultaneous delivery of gene and chemotherapeutics via copolymeric micellar nanoparticles to overcome multiple drug resistance to promote synergistic tumor suppression. Journal of Biomaterials Applications, 2019, 34, 130-140.	2.4	5
155	Effective tumor vessel barrier disruption mediated by perfluoro- <i>N</i> -(4-methylcyclohexyl) piperidine nanoparticles to enhance the efficacy of photodynamic therapy. Nanoscale, 2021, 13, 13473-13486.	5.6	5
156	Sublingual injection of microparticles containing glycolipid ligands for NKT cells and subunit vaccines induces antibody responses in oral cavity. Carbohydrate Research, 2015, 405, 87-92.	2.3	4
157	A Barcoded Polymer-Based Cross-Reactive Spectroscopic Sensor Array for Organic Volatiles. Sensors, 2019, 19, 3683.	3.8	4
158	Education and Outreach in Physical Sciences in Oncology. Trends in Cancer, 2021, 7, 3-9.	7.4	4
159	Constructing helical nanowires <i>via</i> polymerization-induced self-assembly. RSC Advances, 2021, 11, 8986-8992.	3.6	4
160	Cancer Therapy: Cooperative, Nanoparticleâ€Enabled Thermal Therapy of Breast Cancer (Adv. Healthcare) Tj ETC	Qq0.0.0 rg 7.6	BT ¦Overlock
161	Identification of an Inhibitory Mechanism of Luteolin on the Insulinâ€Like Growth Factorâ€1 Ligand–Receptor Interaction. ChemBioChem, 2013, 14, 929-933.	2.6	3

Effective Concentration of a Multikinase Inhibitor within Bone Marrow Correlates with <i>In Vitro</i> Cell Killing in Therapy-Resistant Chronic Myeloid Leukemia. Molecular Cancer Therapeutics, 2016, 15, 899-910.

#	Article	IF	CITATIONS
163	Synthesis and pharmacological evaluation of naftopidil-based arylpiperazine derivatives containing the bromophenol moiety. Pharmacological Reports, 2020, 72, 1058-1068.	3.3	3
164	Nano encapsulated novel compound SA-10 with therapeutic activity in both acute and chronic murine hindlimb ischemia models. Nanomedicine: Nanotechnology, Biology, and Medicine, 2021, 35, 102400.	3.3	3
165	Vulnerable Atherosclerotic Plaque Imaging by Smallâ€Molecule Highâ€Affinity Positron Emission Tomography Radiopharmaceutical. Advanced Therapeutics, 2019, 2, 1900005.	3.2	2
166	Constructing Cylindrical Nanostructures Via Directional Morphology Evolution Induced by Seeded Polymerization. Macromolecular Rapid Communications, 2021, 42, 2100001.	3.9	2
167	Electrochemiluminescence sensing platform for microorganism detection. Biosafety and Health, 2022, 4, 61-63.	2.7	2
168	Rad51 Silencing with siRNA Delivered by Porous Silicon-Based Microparticle Enhances the Anti-Cancer Effect of Doxorubicin in Triple-Negative Breast Cancer. Journal of Biomedical Nanotechnology, 2021, 17, 2351-2363.	1.1	2
169	An Enhanced Photothermal Therapeutic Iridium Hybrid Platform Reversing the Tumor Hypoxic Microenvironment. Molecules, 2022, 27, 2629.	3.8	2
170	Tracking Biodistribution of Myeloid-Derived Cells in Murine Models of Breast Cancer. Genes, 2019, 10, 297.	2.4	1
171	Identification of an Aptamer With Binding Specificity to Tumor-Homing Myeloid-Derived Suppressor Cells. Frontiers in Pharmacology, 2021, 12, 752934.	3.5	1
172	Binding model-tuned room-temperature phosphorescence of the bromo-naphthol derivatives based on cyclodextrins. RSC Advances, 2022, 12, 19313-19316.	3.6	1
173	Surface Engineering and Multimodal Imaging of Multistage Delivery Vectors in Metastatic Breast Cancer. Bio-protocol, 2021, 11, e4030.	0.4	0
174	A heparan-sulfate-bearing syndecan-1 glycoform is a distinct surface marker for intra-tumoral myeloid-derived suppressor cells. IScience, 2021, 24, 103349.	4.1	0
175	Antitumor Immunity from Abdominal Flap-Embedded Therapeutic Cancer Vaccine. International Journal of Nanomedicine, 2022, Volume 17, 203-212.	6.7	0